

Supporting Information for:

## **SO<sub>2</sub> Capture and Detection by Cu(II)-Metal Organic Polyhedron**

Eva Martínez-Ahumada,<sup>†a</sup> Alfredo López-Olvera,<sup>†\*a</sup> Paulina Carmona-Monroy,<sup>a</sup> Howard Díaz-Salazar,<sup>b</sup> Monserrat H. Garduño-Castro,<sup>c</sup> Juan L. Obeso,<sup>d</sup> Carolina Leyva,<sup>d</sup> Ana Martínez,<sup>e</sup> Marcos Hernández-Rodríguez,<sup>b</sup> Diego Solis-Ibarra,<sup>\*,a</sup> and Ilich A. Ibarra<sup>\*,a</sup>

<sup>a</sup>Laboratorio de Fisicoquímica y Reactividad de Superficies (LaFRoS), Instituto de Investigaciones en Materiales, Universidad Nacional Autónoma de México, Circuito Exterior s/n, CU, Del Coyoacán, 04510, México D.F., México.

<sup>b</sup>Instituto de Química, Universidad Nacional Autónoma de México, Circuito Exterior, Ciudad Universitaria, Del. Coyoacán, C. P. 04510, Cd. Mx., México.

<sup>c</sup>Sygnature Discovery, Alderly Park, Alderly Edge, Cheshire SK10 4TG, United Kingdom.

<sup>d</sup>Instituto Politécnico Nacional, Centro de Investigación en Ciencia Aplicada y Tecnología Avanzada, Calz. Legaria 694, Col. Irrigación, Miguel Hidalgo, 11500, CDMX, México.

<sup>e</sup>Departamento de Materiales de Baja Dimensionalidad. Instituto de Investigaciones en Materiales, and Facultad de Química, Universidad Nacional Autónoma de México Circuito Exterior s/n, CU, Del. Coyoacán, Ciudad de México 04510, México.

## Table of Contents

<b>S1. Experimental details</b> .....	S3
<b>S2. Characterization of MOP-CDC</b> .....	S4
<b>S3. Results and discussion</b> .....	S6
<b>S4. References</b> .....	S12

## S1. Experimental Details

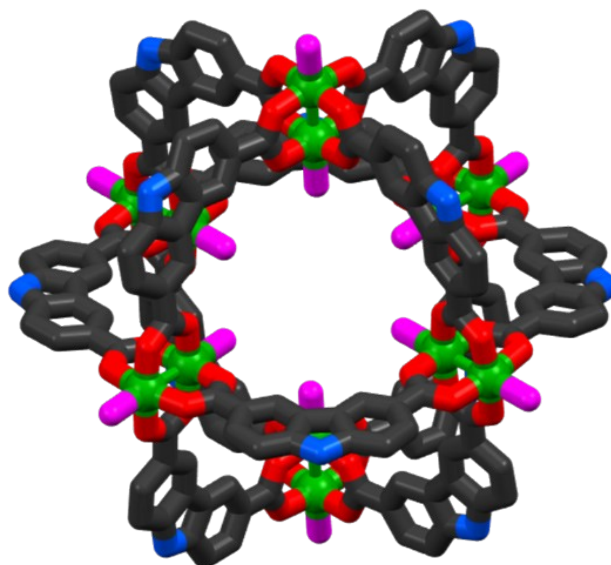
### Materials synthesis

Pentahydrate copper nitrate ( $\text{Cu}(\text{NO}_3)_2 \cdot 5\text{H}_2\text{O}$ ,  $\geq 98\%$ ), *N,N*-dimethylformamide (DMF,  $\geq 99.8\%$ ), and ethanol ( $\text{EtOH}$ ,  $\geq 99.8\%$ ), were supplied by Sigma-Aldrich. All reagents and solvents were used as received from commercial suppliers without further purification.

The  $\text{SO}_2$  isotherms were recorded at 298 K and up to 1 bar with the aid of a Dynamic Gravimetric Gas/Vapour Sorption Analyser, DVS Vacuum (Surface Measurements Systems Ltd.). Ultra-pure grade (99.9995%)  $\text{SO}_2$  were purchased from PRAXAIR.

### Synthesis of MOP-CDC

MOP-CDC was synthesized according to literature<sup>1</sup>. A mixture of 9*H*-carbazole-3,6-dicarboxylic acid ( $\text{H}_2\text{CDC}$ ), (8 mg, 0.031 mmol) and  $\text{Cu}(\text{NO}_3)_2 \cdot 5\text{H}_2\text{O}$  (4.8 mg, 0.022 mmol) in DMF/EtOH 1:1 (1.5 mL) was heated up at 120° C for 24 h. The result blue-green crystals were washed with fresh ethanol for 3 days (yield 9.2 mg 67%).



**Scheme S1.** Structure of MOP-CDC along the *a*-axis showing the 13.8 Å cavity and the window-pore with 11.9 Å gap.<sup>1</sup> Atom label: green sphere: copper; black: carbon; red: oxygen; blue: nitrogen; pink: coordinated solvent (DMF)

## S2. Characterization of MOP-CDC

### Powder X-Ray Diffraction Patterns (PXRD)

The PXRD were recorded on a Rigaku Diffractometer, Ultima IV with a Cu-K $\alpha_1$  radiation ( $\lambda = 1.5406 \text{ \AA}$ ) using a nickel filter. Patterns were recorded in the 5–40° 2 $\theta$  range with a step scan of 0.02° and a scan rate of 0.08° min<sup>-1</sup>.

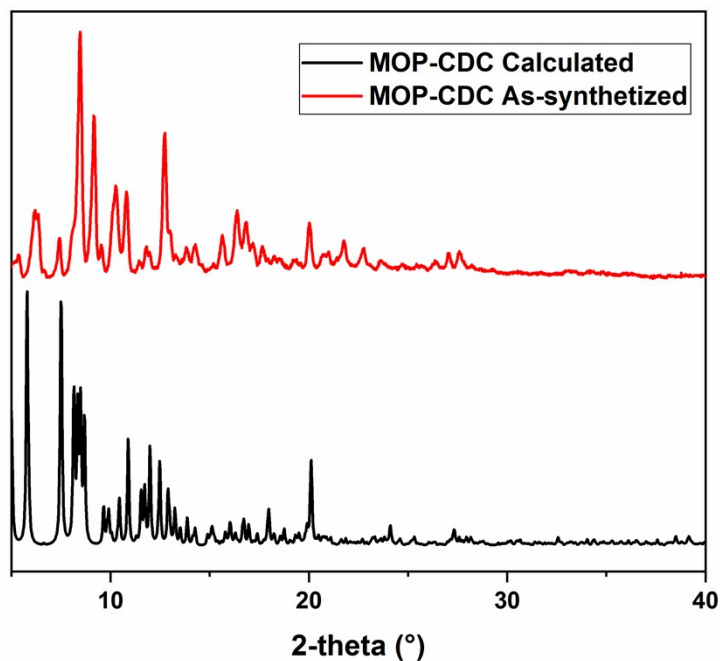


**Figure S1.** Powder X-ray diffraction (PXRD) patterns for as-MOP-CDC, the experimental (red line) and calculated (black line).

## Fourier Transform Infrared Spectroscopy (FT-IR)

FT-IR spectra were obtained in the range of 4000-400  $\text{cm}^{-1}$  on a Bruker Tensor 27 spectrometer with a Golden Gate Single Reflection diamond ATR cell.

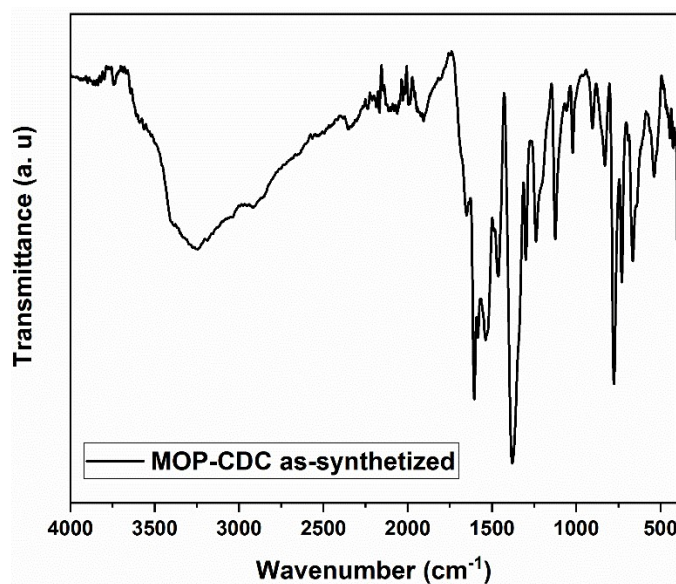


**Figure S2.** The FT-IR spectra of as-synthesized MOP-CDC.

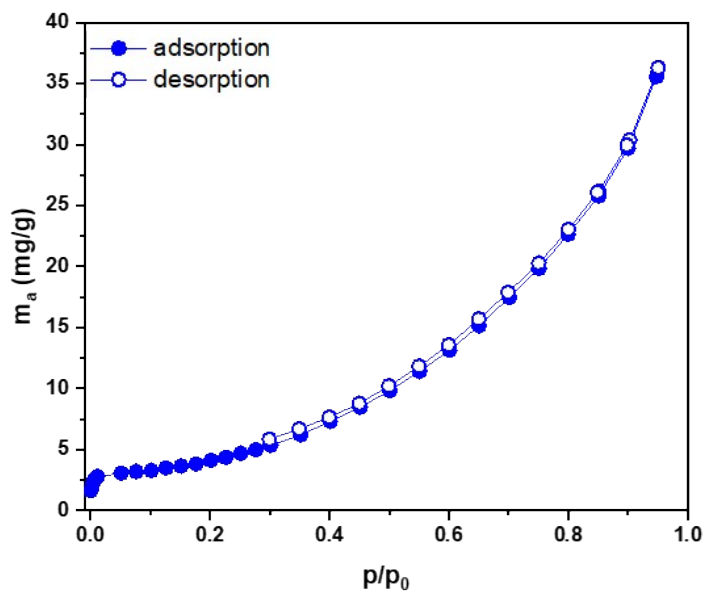


**Figure S3.**  $\text{N}_2$  adsorption isotherm of MOP-CDC at 77 K.



### S3. Results and discussion

#### Characterization of MOP-CDC before and after SO<sub>2</sub> adsorption-desorption experiments

#### FT-IR spectra of MOP-CDC before and after SO<sub>2</sub> adsorption-desorption experiments

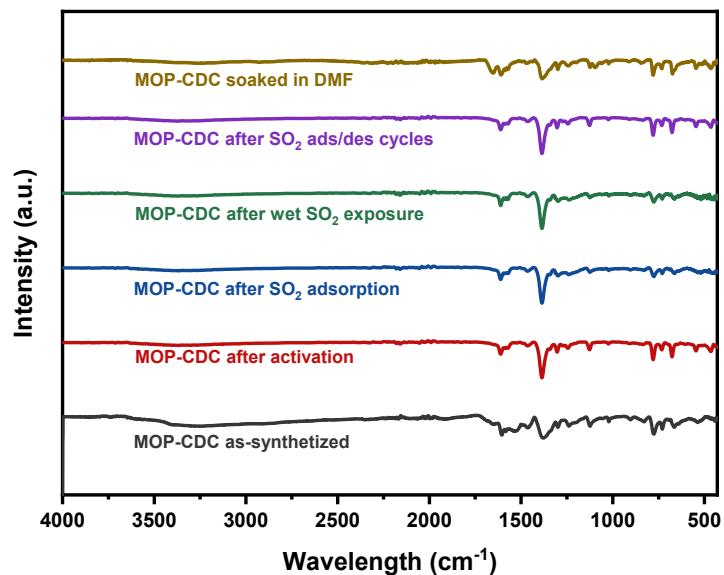
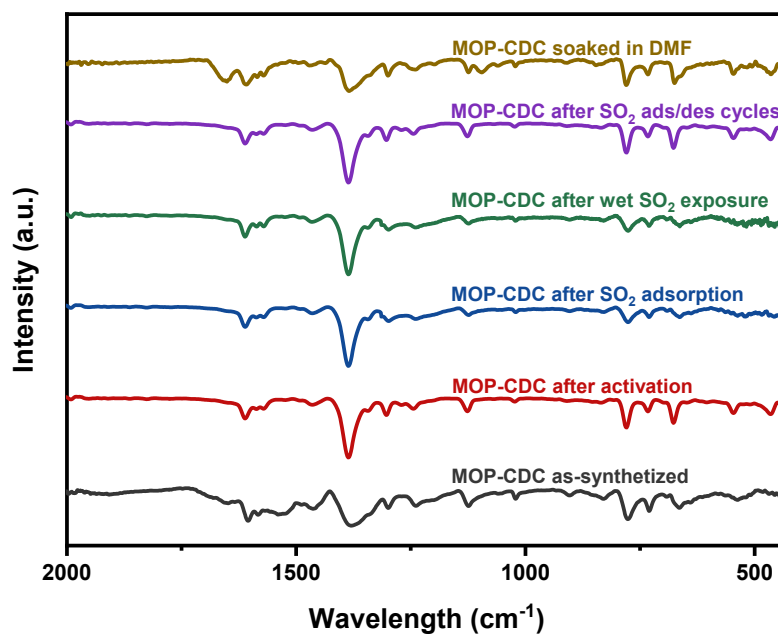


**Figure S4.** The FT-IR spectra of MOP-CDC as-synthesized (black line), after activation (red line), after SO<sub>2</sub> adsorption (blue line), after wet SO<sub>2</sub> exposure (green line), after SO<sub>2</sub> ads/des cycles (purple line) and soaked in DMF (yellow line).

**Figure S5.** Inset (2000-500  $\text{cm}^{-1}$ ) of FT-IR spectra of MOP-CDC as-synthesized (black line), after activation (red line), after  $\text{SO}_2$  adsorption (blue line), after wet  $\text{SO}_2$  exposure (green line), after  $\text{SO}_2$  ads/des cycles (purple line) and soaked in DMF (yellow line).



**PXRD patterns after activation,  $\text{SO}_2$  adsorption, and soaked in DMF**

**Figure S6.** The PXRD patterns of MOP-CDC as-synthesized (black line), after activation (red line), after SO<sub>2</sub> adsorption (blue line), and soaked in DMF (green line).

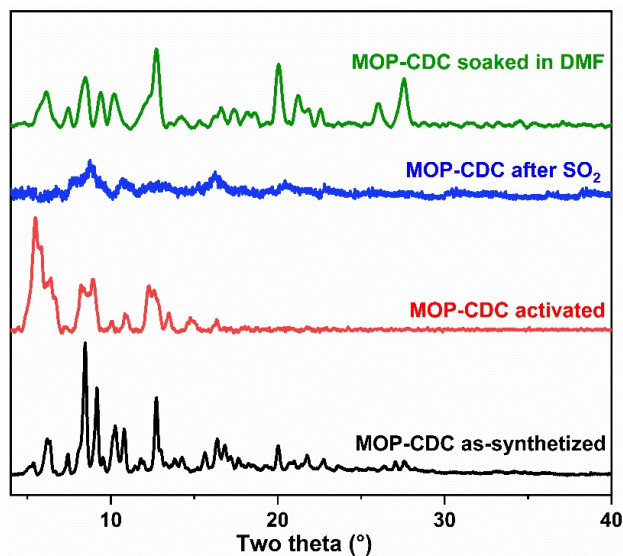


**Table S1.** SO<sub>2</sub> adsorption capacity of some related MOFs with BET surface area similar.

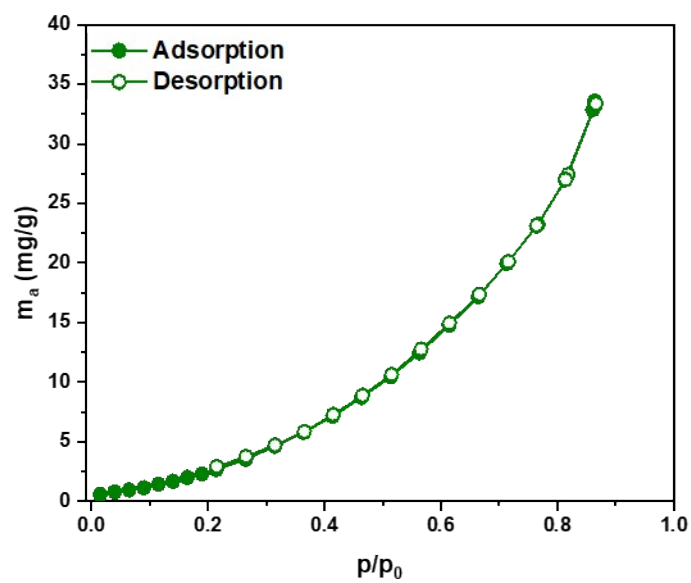
**Table S1.** SO<sub>2</sub> adsorption capacity of some related MOFs with BET surface area similar.

MOFs	SO <sub>2</sub> uptake (mmol g <sup>-1</sup> ) at 298 and 0.05	BET Surface area (m <sup>2</sup> g <sup>-1</sup> )	Pore Volume (cm <sup>3</sup> g <sup>-1</sup> )	SO <sub>2</sub> interaction	Ref.

<b>bar</b>						
MOP-CDC	1.0	-	-	N-H...O=S=O		
				Weak interaction (hydrogen bonding)		2
NU-1000	1.2	1970	1.196			
Co-URJC-5	0.8	223	1.32*	Py...SO <sub>2</sub>		3
MOF-177	1.1	4100	1.51	chemical instability to SO <sub>2</sub>		4
			0.84	sulfur atoms with paddlewheel metal oxygen carbon units		5
Zn(bdc)(ted) <sub>0.5</sub>	1.2	1783				
DUT-4	2.4	1348	1.71	μ-OH adsorption site		6
MIL-53(Al)-BDC	0.6	1210	0.51	μ-OH adsorption site by breathing behaviour		7

\*from crystal density

**Figure S7.** N<sub>2</sub> adsorption isotherm of MOP-CDC at 77 K after SO<sub>2</sub> adsorption studies.



### Isosteric heat of SO<sub>2</sub> adsorption experiments

Heat of adsorption of MOP-CDC was calculated accordingly to reported literature,<sup>9</sup> using a virial-type equation (Eq. S2) to fit the low coverage region of two adsorption isotherms at 298 and 308 K (Figure S8).

$$\ln(n/p) = A_0 + A_1\eta + A_2\eta^2 + \dots \quad \text{Eq. S2}$$

Where  $p$  is the pressure,  $n$  is the amount adsorbed and  $A_0, A_1, \dots$  are the virial coefficients. The plot of  $\ln(n/p)$  give a straight line at low surface coverage (Figure S9). From the linear fittings (using the Clausius-Clapeyron equation) the virial coefficients are used to estimate the enthalpy of adsorption. The obtained value was  $44.8 \text{ kJ mol}^{-1}$

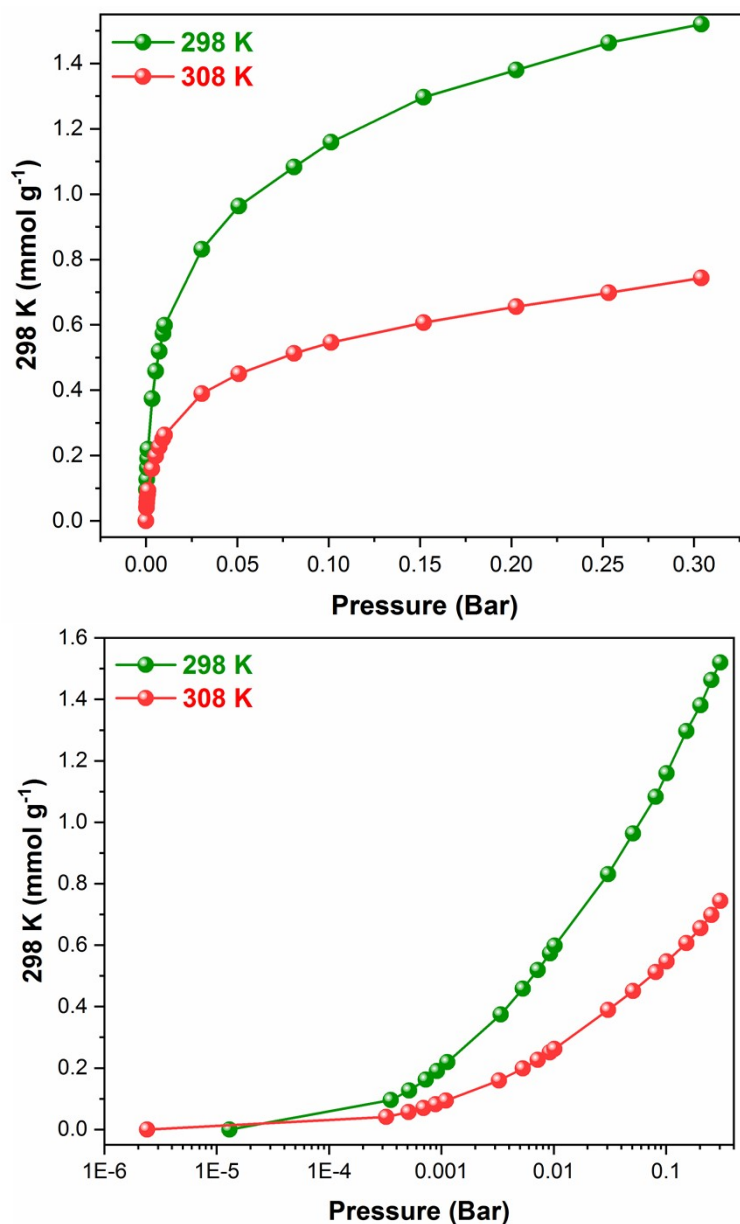


**Figure S8.** SO<sub>2</sub> adsorption isotherms of MOP-CDC. at 298 and 308 K.

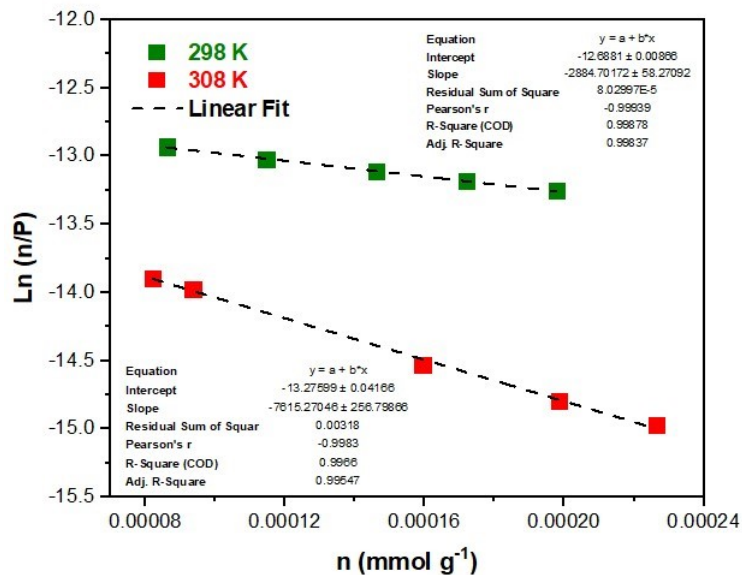


**Figure S9.** Virial fitting plots for the adsorption isotherms of SO<sub>2</sub> for MOP-CDC.

### DFT computational studies

The model represents the structure of the MOP-CDC. To comply with the valence, we include CH<sub>3</sub> groups attached to the oxygen atoms. This model is not optimized since we want to represent the experimental structure. The SO<sub>2</sub> was originally bound to different atoms of the MOP (Cu, CH and NH). Only the SO<sub>2</sub> molecule was optimized. Gaussian09 was used for all electronic calculations.<sup>13</sup> Partial geometry optimizations were performed at B3LYP/LAND2DZ level of theory.<sup>14,15</sup>

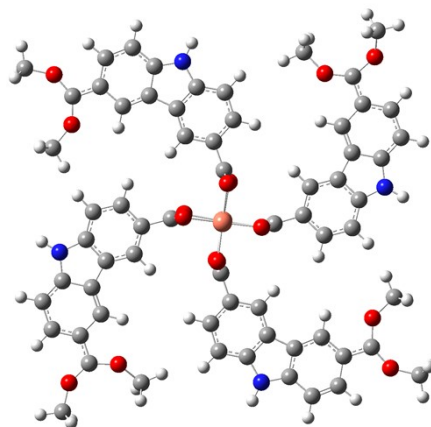


**Figure S10.** Calculated fraction structure of MOP-CDC.

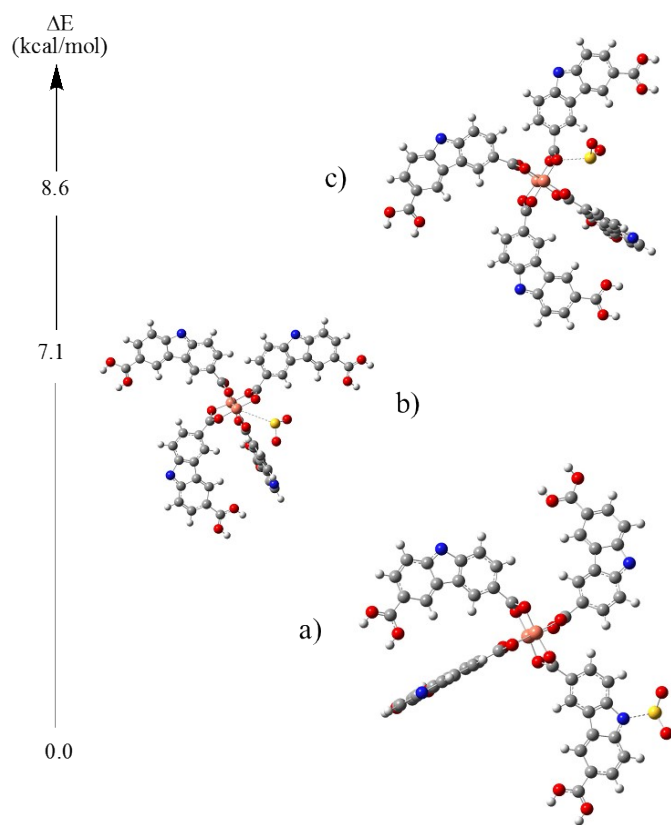


**Figure S11.** Interaction of SO<sub>2</sub> by S atom with different sites of MOP-CDC, a) NH , b) Cu and c) O<sub>carboxylate</sub>.

**Figure S12.** Optimized structures. The most stable interaction is with NH. Energy interaction is 44.1 Kcal/mol.

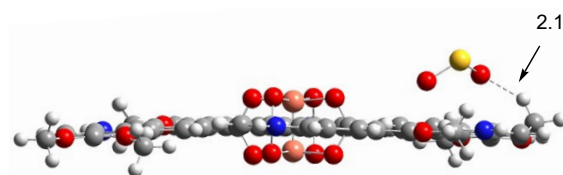
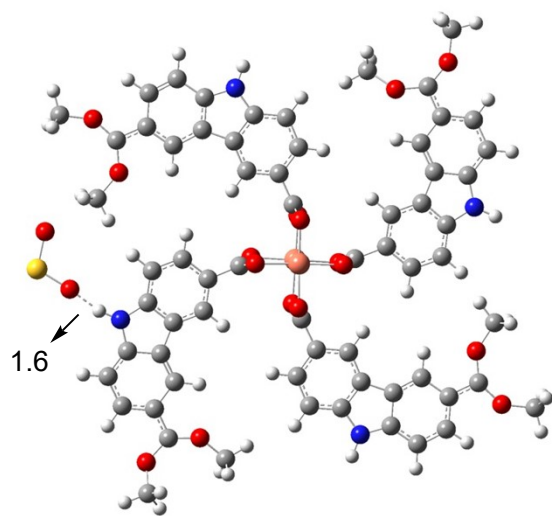
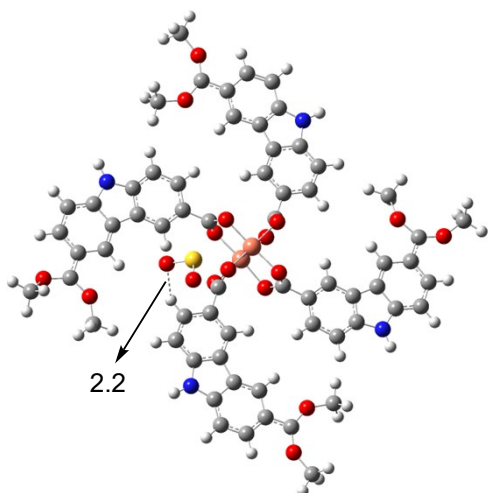


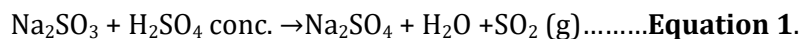
**Figure S13.** Optimized structures. The interaction with CH<sub>3</sub> is 10.3 kcal/mol less stable



### System for *in situ* SO<sub>2</sub> exposure experiments

**Figure S14.** Optimized structures. There is another stable interaction that is 21.6 Kcal/mol less stable than the system adapted from the reported literature.<sup>8</sup> The system contains two principal parts: SO<sub>2</sub> gas generator (A) dropping funnel with H<sub>2</sub>SO<sub>4</sub> conc. [1] connected to a Schlenk flask with Na<sub>2</sub>SO<sub>3</sub> (s) under stirring [2]; and the saturation chamber (B), constructed from a round flask with distilled water [3], connected to a sintered glass filter adapter [4] and to a vacuum line [5]. The activated sample is placed on the glass filter adapter.

Considering the molar reaction (Eq. 1), we assume that the SO<sub>2</sub> flow was the 50 ppm min<sup>-1</sup>, since we have added 0.2 mL of concentrated sulphuric acid to an enough sodium sulphite. The activated MOP-CDC sample was tested at this flow (50 ppm min<sup>-1</sup>) for 24 h and immediately PXRD, FT-IT, UV and PL experiments were recorded. In the case of anhydrous experiments (to exclude the water affect) a sulphuric acid trap was used.



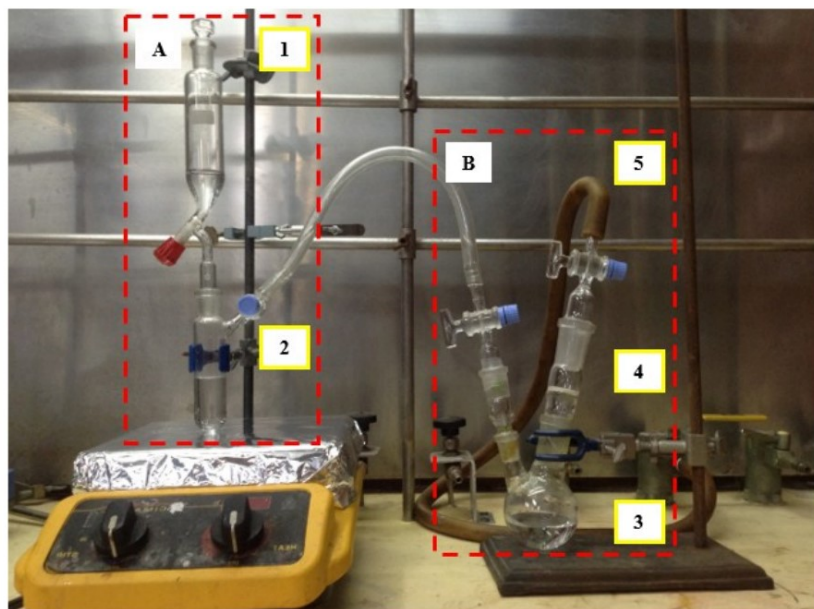
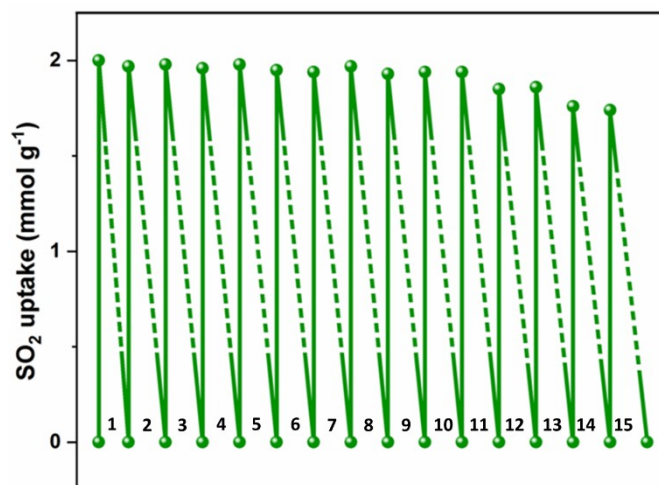


**Figure S15.** Homemade system for wet SO<sub>2</sub> adsorption experiments.

**SO<sub>2</sub> cyclability assessment**

**Figure S16.** Experimental fifteen SO<sub>2</sub> adsorption-desorption (solid and dashed line, respectively) cycles from 0 to 1 bar with dynamic vacuum ( $1.7 \times 10^{-6}$  torr) for MOP-CDC.



#### **Effect of extrinsic porosity in the SO<sub>2</sub> adsorption properties.**

In order to determine the effect of the extrinsic porosity formed by the voids between each MOP-CDC motifs (crystal lattice), we have amorphized two independent MOP-CDC samples using an Agatha mortar (Figure S17). Then, two new SO<sub>2</sub> adsorption isotherms were recorded with a slight decrement close to 15% (figure S18). This abatement is similar to observed in the cyclability experiments after 13 cycle. Additionally, the structure stability of each MOP-CDC was corroborated by FTIR experiments (Figure S19).

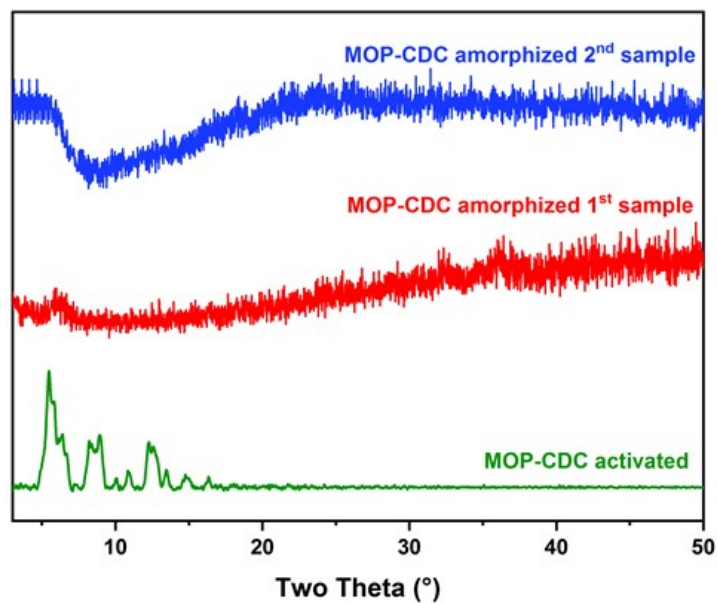


**Figure S17.** PXRD comparison of the MOP-CDC activated (green), MOP-CDC amorphized (first and second samples, red and blue lines, respectively).

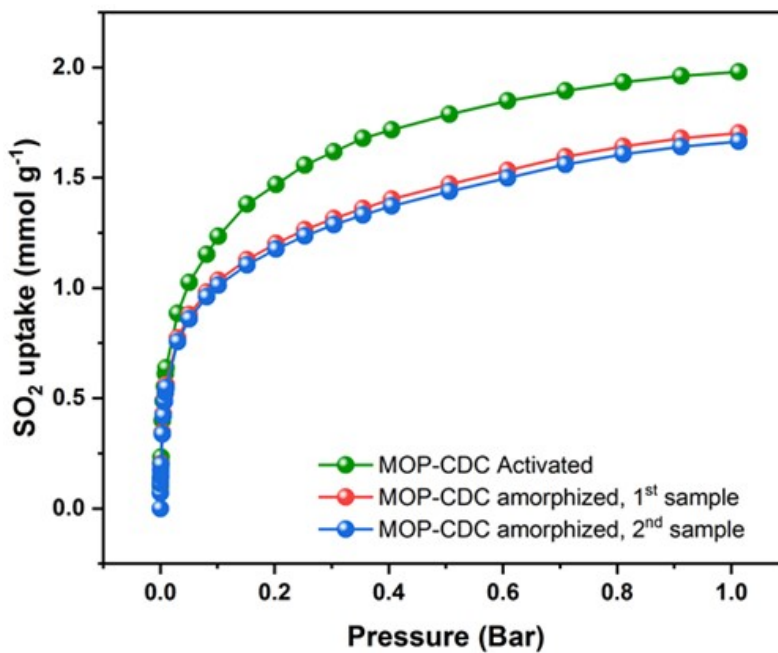


**Figure S18.** SO<sub>2</sub> adsorption isotherm for MOP-CDC activated (green), MOP-CDC amorphized, first sample (red), second sample (blue).

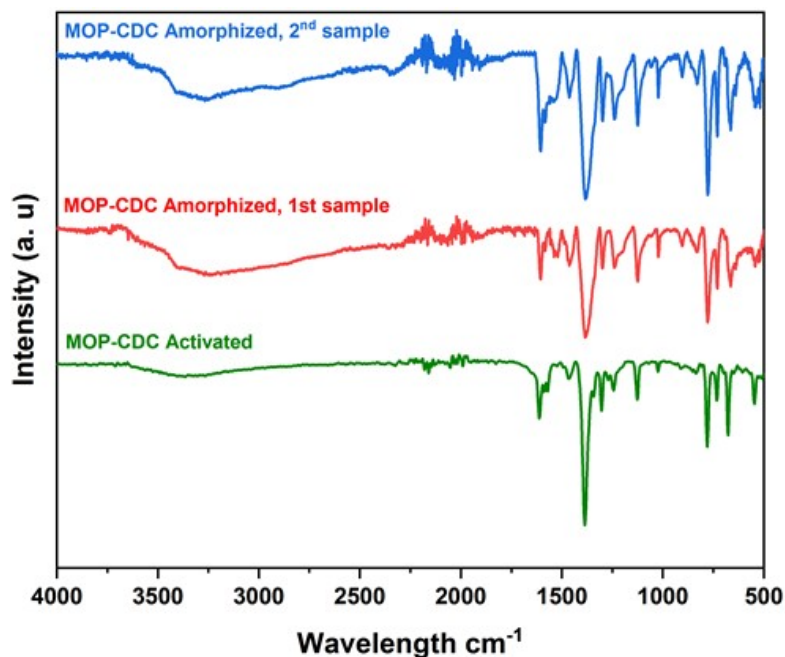


**Figure S19.** FTIR comparison: MOP-CDC activated (green line), MOP-CDC amorphized, first sample (red line), second sample (blue line).

### UV-vis spectra of absorption experiments

Absorption measurements were recorded using a Shimadzu spectrophotometer UV-2600 equipped with an ISR-2600Plus integrating sphere and a BaSO<sub>4</sub> blank.

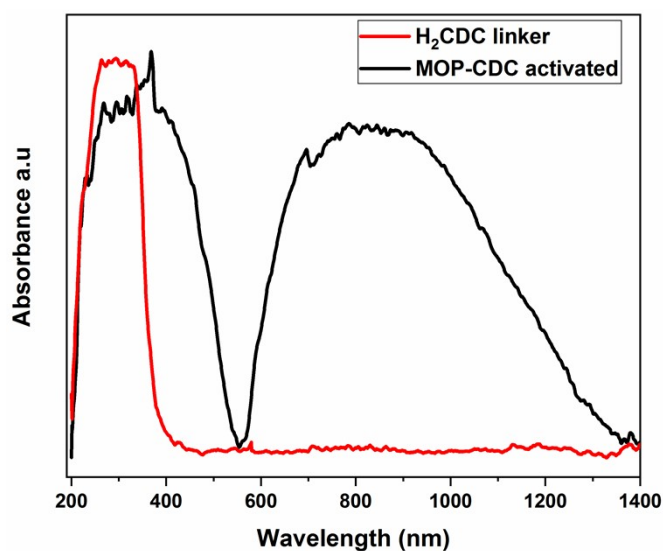
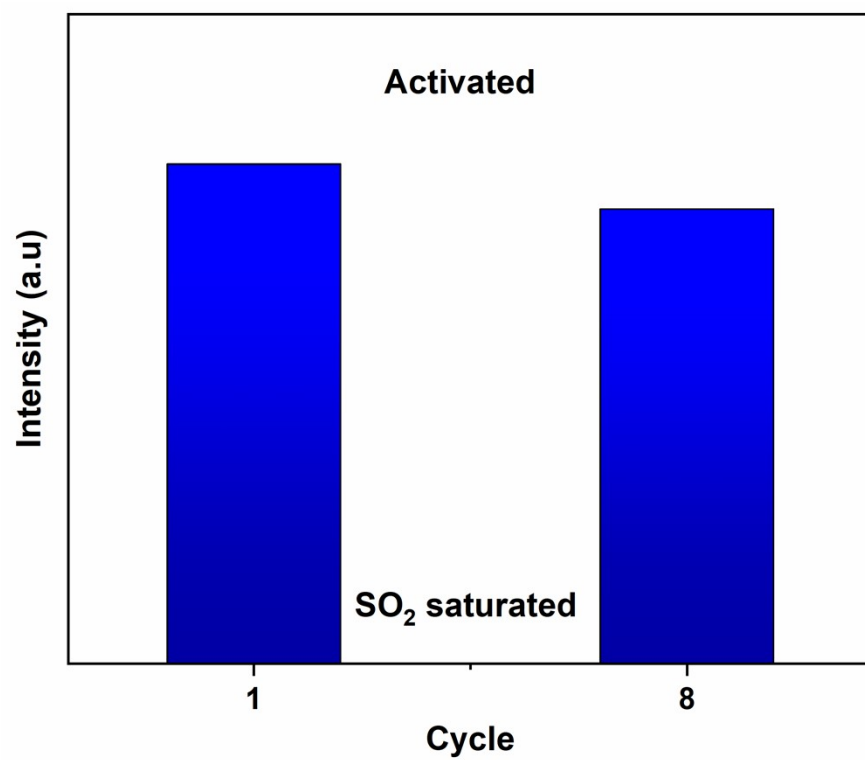


**Figure S20.** Solid state ultraviolet-visible spectroscopy (UV-VIS) spectra of MOP-CDC (black line) and H<sub>2</sub>CDC linker (red line).

## **Photoluminiscent experiments**

Emission spectra were obtained in an Edinburgh Instrument FS5 fluorimeter using a continuous wave 150 W ozone-free xenon arc lamp at room temperature.

**Figure S21.** Cycling fluorescence of activated and SO<sub>2</sub> saturated MOP-CDC (from 1 to 8 cycle).



### CO<sub>2</sub> and H<sub>2</sub>S MOP-CDC sample saturation

According to Zarate and co-workers,<sup>8</sup> using the homemade gas saturator (via supra) an activated MOP-CDC sample was saturated of H<sub>2</sub>S. 0.2 mL per minute of HCl (15%) was added drop wise to Fe<sub>2</sub>S<sub>3</sub> (solid) during 24 h. An Black and white solid were formed into the pan saturator after the H<sub>2</sub>S exposition. In order to examine the MOP-CDC structure, FTIR spectrum after the H<sub>2</sub>S exposition was recorded (Figure 5 orange line). Several new band were observed suggesting that the MOP-CDC structure was collapsed. According to Bandosz and Petit,<sup>10</sup> the H<sub>2</sub>S molecule can interact with the unsaturated copper site to the point of degrading the material and forming CuS specie. This detrimental effect is not only observed in the Cu(II)-Based MOFs but also Hammon and co-worker proved that the MIL-53(Fe) undergoes a structural degradation up to FeS.<sup>11</sup> Then, by washing the crude with heated DMF we could isolate the black powder and a FTIR spectra was recorded (Figure 5, black line), a set of 5 bands were observed which coincide with the reported to the CuS specie.<sup>12</sup> Additional, the MOP-CDC after H<sub>2</sub>S exposition and the H<sub>2</sub>CDC linker (Figure 5, orange and blue lines) matched in several bands, especially the carboxylate band were observed. Taking into an account these finding, we confirm that the MOP-CDC is not stable toward H<sub>2</sub>S atmosphere, thereby not new fluorimetric analysis have not been carried out using H<sub>2</sub>S as probe molecule.

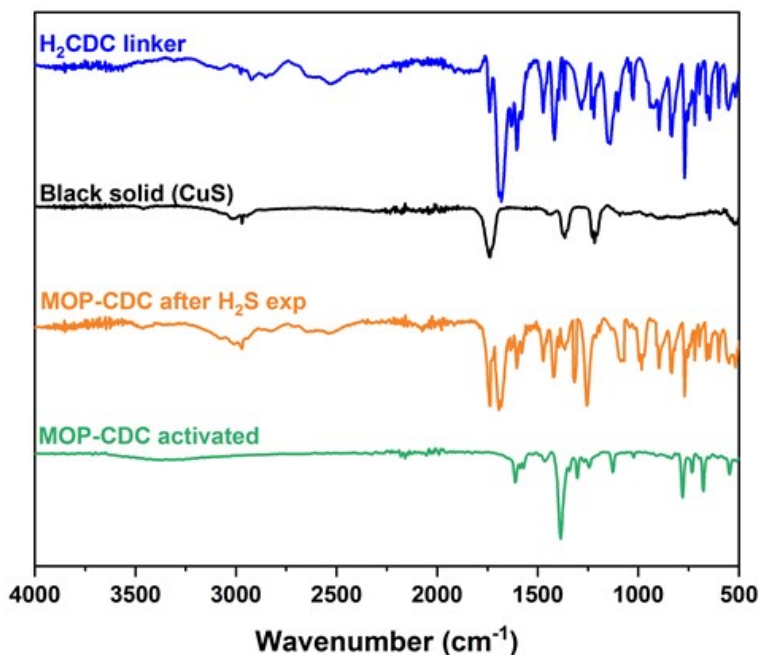


**Figure S22.** FTIR comparison of MOP-CDC activated (green line), MOP-CDC after H<sub>2</sub>S (orange line), Black solid (black line), as-H<sub>2</sub>CDC linker (blue line).

#### S4. References

- 1 A. López-Olvera, E. Sánchez-González, A. Campos-Reales-Pineda, A. Aguilar-Granda, I. A. Ibarra and B. Rodríguez-Molina, *Inorg. Chem. Front.*, 2017, **4**, 56–64.
- 2 S. Gorla, M. L. Díaz-Ramírez, N. S. Abeynayake, D. M. Kaphan, D. R. Williams, V. Martis, H. A. Lara-García, B. Donnadieu, N. Lopez, I. A. Ibarra and V. Montiel-Palma, *ACS Appl. Mater. Interfaces*, 2020, **12**, 41758–41764.
- 3 A. López-Olvera, H. Montes-Andrés, E. Martínez-Ahumada, V. B. López-Cervantes, R. D. Martínez-Serrano, E. González-Zamora, A. Martínez, P. Leo, C. Martos, I. A. Ibarra and G. Orcajo, *Eur. J. Inorg. Chem.*, 2021, **2021**, 4458–4462.
- 4 P. Brandt, A. Nuhnen, M. Lange, J. Möllmer, O. Weingart and C. Janiak, *ACS Appl. Mater. Interfaces*, 2019, **11**, 17350–17358.
- 5 K. Tan, P. Canepa, Q. Gong, J. Liu, D. H. Johnson, A. Dyevoich, P. K. Thallapally, T. Thonhauser, J. Li and Y. J. Chabal, *Chem. Mater.*, 2013, **25**, 4653–4662.
- 6 A. López-Olvera, S. Pioquinto-García, J. Antonio Zárate, G. Diaz, E. Martínez-Ahumada, J. L. Obeso, V. Martis, D. R. Williams, H. A. Lara-García, C. Leyva, C. V. Soares, G. Maurin, I. A. Ibarra and N. E. Dávila-Guzmán, *Fuel*, 2022, **322**, 124213.
- 7 A. López-Olvera, J. Antonio Zárate, E. Martínez-Ahumada, D. Fan, M. L. Díaz-Ramírez, P. A. Sáenz-Cavazos, V. Martis, D. R. Williams, E. Sánchez-González, G. Maurin and I. A. Ibarra, *ACS Appl. Mater. & Interfaces*, 2021, **13**, 39363–39370.
- 8 A. Nuhnen and C. Janiak, *Dalt. Trans.*, 2020, **49**, 10295–10307.
- 9 Frisch, M. J.; Trucks, G. W.; Schlegel, H. B.; Scuseria, G. E.; Robb, M. A.; Cheeseman, J. R.; Montgomery, J. J. A.; Vreven, T.; Kudin, K. N.; Burant, J. C.; Millam, J. M.; Iyengar, S. S.; Tomasi, J.; Barone, V.; Mennucci, B.; Cossi, M.; Scalmani, G.; Rega, N.; Petersson, G. A.; Nakatsuji, H.; Hada, M.; Ehara, M.; Toyota, K.; Fukuda, R.;

Hasegawa, J.; Ishida, M.; Nakajima, T.; Honda, Y.; Kitao, O.; Nakai, H.; Klene, M.; Li, X.; Knox, J. E.; Hratchian, H. P.; Cross, J. B.; Bakken, V.; Adamo, C.; Jaramillo, J.; Gomperts, R.; Stratmann, R.E.; Yazyev, O.; Austin, A. J.; Cammi, R.; Pomell, C.; Ochterski, J. W.; Ayala, P. Y.; Morokuma, K.; Voth, G. A.; Salvador, P.; Dannenberg, J. J.; Zakrzewski, V. G.; Dapprich, S.; Daniels, A. D.; Strain, M. C.; Farkas, O.; Malick, D. K.; Rabuck, A. D.; Raghavachari, K.; Foresman, J. B.; Ortiz, J. V.; Cui, Q.; Baboul, A. G.; Clifford, S.; Cioslowski, J.; Stefanov, B. B.; Liu, G.; Liashenko, A.; Piskorz, P.; Komaromi, I.; Martin, R. L.; Fox, D. J.; Keith, T.; Al-Laham, M. A.; Peng, C. Y.; Nanayakkara, A.; Challacombe, M.; Gill, P. M. W.; Johnson, B.; Chen, W.; Wong, M. W.; Gonzalez, C.J.; Pople, A. *Gaussian 09*, Revision A.08, Inc. Wallingford, CT, **2009**

- 10 Alex D. Beck, *J. Chem. Phys.*, 1993, **98**, 5648–5656.
- 11 P. J. Hay and W. R. Wadt, *J. Chem. Phys.*, 1985, **82**, 270–283.
- 12 S. Van Mileghem and W. M. De Borggraeve, *Org. Process Res. Dev.*, 2017, **21**, 785–787.
- 13 C. Petit, B. Mendoza and T. J. Bandosz, *ChemPhysChem*, 2010, **11**, 3678–3684.
- 14 L. Hamon, C. Serre, T. Devic, T. Loiseau, F. Millange, G. Férey and G. De Weireld, *J. Am. Chem. Soc.*, 2009, **131**, 8775–8777.
- 15 P. Naveenkumar, G. Paruthimal Kalaignan, S. Arulmani and S. Anandan, *J. Mater. Sci. Mater. Electron.*, 2018, **29**, 16853–16863.